Rock Mech Rock Eng (2018) 51:911–923
https://doi.org/10.1007/s00603-017-1353-5

ORIGINAL PAPER

Thermal Properties of Consolidated Granular Salt as a Backfill Material

Laxmi P. Paneru[1] · Stephen J. Bauer[2] · John C. Stormont[1]

Received: 19 January 2017 / Accepted: 28 October 2017 / Published online: 11 November 2017

Abstract Granular salt has been proposed as backfill material in drifts and shafts of a nuclear waste disposal facility where it will serve to conduct heat away from the waste to the host rock. Creep closure of excavations in rock salt will consolidate (reduce the porosity of) the granular salt. This study involved measuring the thermal conductivity and specific heat of granular salt as a function of porosity and temperature to aid in understanding how thermal properties will change during granular salt consolidation accomplished at pressures and temperatures consistent with a nuclear waste disposal facility. Thermal properties of samples from laboratory-consolidated granular salt and in situ consolidated granular salt were measured using a transient plane source method at temperatures ranging from 50 to 250 °C. Additional measurements were taken on a single crystal of halite and dilated polycrystalline rock salt. Thermal conductivity of granular salt decreased with increases in temperature and porosity. Specific heat of granular salt at lower temperatures decreased with increasing porosity. At higher temperatures, porosity dependence was not apparent. The thermal conductivity and specific heat data were fit to empirical models and compared with results presented in the literature. At comparable densities, the thermal conductivities of granular salt samples consolidated hydrostatically in this study were greater than those measured previously on samples formed by quasi-static pressing. Petrographic studies of the consolidated salt indicate that the consolidation method influenced the nature of the porosity; these observations are used to explain the variation of measured thermal conductivities between the two consolidation methods. Thermal conductivity of dilated polycrystalline salt was lower than consolidated salt at comparable porosities. The pervasive crack network along grain boundaries in dilated salt impedes heat flow and results in a lower thermal conductivity compared to hydrostatically consolidated salt.

Keywords Rock salt · Thermal properties · Backfill · Consolidation · Porosity

1 Introduction

Nuclear wastes are generated worldwide that require safe and permanent disposal. For example, in the USA decades of commercial nuclear power production and nuclear weapons production have resulted in a growing inventory of spent nuclear fuel and other high-level nuclear wastes that are being temporarily stored (National Research Council 2001). Salt formations have several favourable attributes as a host medium for nuclear waste disposal. The existence of massive, stable salt formations and their low permeability indicates they are effectively isolated from groundwater (Beauheim and Roberts 2002; Cosenza et al. 1999). Salt creeps plastically which results in the closure of shafts and tunnels, and eventually entombs the waste (Carter and Hansen 1983). Salt is also an excellent conductor of heat and will tend to dissipate heat generated from the waste (Martin et al. 2015).

Salt formations are currently being used as a medium for some radioactive waste disposal. In the USA, the Waste Isolation Pilot Plant (WIPP), constructed in a bedded salt formation in Southeastern New Mexico, is storing

✉ John C. Stormont
jcstorm@unm.edu

[1] Department of Civil Engineering, University of New Mexico, Albuquerque, NM 87131, USA

[2] Geomechanics Department, Sandia National Laboratories, P.O. Box 5800, Albuquerque, NM 87185-1033, USA

defence-generated transuranic wastes (Conca et al. 2005). In Germany, radioactive wastes have been stored in the Endlager für radioaktive Abfälle Morsleben (ERAM) domal salt site in Morsleben, Germany (von Berlepsch and Haverkamp 2016). The Asse II salt dome mine in Germany received some low-level and intermediate-level radioactive waste from 1967 to 1978 for research purposes (Damveld and Bannink 2012).

Granular salt, a by-product of excavation, has been proposed to be used as backfill material in drifts and shafts of a disposal facility (e.g. Bechthold et al. 1999). Creep closure of the formation surrounding the excavation will exert pressure on the placed granular salt and eventually consolidate it into a density comparable to intact polycrystalline salt. The time-dependent consolidation of granular salt can reduce its porosity from 0.4 in a loose state to an eventual end state of less than 0.01. Granular salt backfill will conduct heat away from the waste to the host rock as well as distribute the compressive load of surrounding formation onto the waste canisters (Bechthold et al. 1999). Elevated temperatures in the vicinity of heat generating waste will increase consolidation rates (Hansen et al. 2014). Owing to the dramatic impact that water has on accelerating consolidation (Hansen et al. 2014; Stormont and Finley 1996), a small amount of water will likely be added to granular salt as it is emplaced.

Because thermal properties of porous media are a function of porosity (Woodside and Messmer 1961a, b), the thermal properties of granular salt are expected to change during consolidation. In particular, porosity has a significant effect on the thermal conductivity, with the magnitude of the effect dependent on the arrangement of the pore space (Durham and Abey 1981). An understanding of how thermal properties change during consolidation is necessary to predict how a repository will respond to the heat generated from radioactive waste.

Thermal properties of single-crystal halite are known to be a function of temperature (Birch and Clark 1940; Smith 1976; Acton 1977; Sweet and McCreight 1979; Urquhart and Bauer 2015). Urquhart and Bauer (2015) report the thermal conductivity of single-crystal halite decreased with increasingtemperature, varying from 9.975 W/m K at − 75 °C to 2.699 W/m K at 300 °C. This presumably is the result of thermal expansion of the crystal lattice, reducing the conduction process. For polycrystalline salt, thermal properties have been found to be a function of composition of impurities (Durham and Abey 1981; Acton 1977; Sweet and McCreight 1979; van den Broek 1982), grain size (Bechthold et al. 1999), porosity (Bauer and Urquhart 2015), as well as temperature.

Bauer and Urquhart (2015) measured thermal properties on granular salt at various porosities and temperatures up to 300 °C. They sieved granular salt from the WIPP to obtain grain sizes less than 9.5 mm. The granular salt samples were then compacted in a die (essentially uniaxial strain condition) and compressed to form a pellet (sample) of 50 mm in diameter and 25 mm in height; the load on the samples when pressed was not specifically recorded but was in the range of 40–50 MPa. No water was added to the salt. Mass and volume of the pellets were measured to calculate bulk densities and compared with the known grain density of crushed salt (2.14 g/cc). Porosity was calculated as:

$$\phi = 1 - \frac{\rho_B}{\rho_G} \tag{1}$$

where ρ_B is bulk density (g/cc) and ρ_G is salt grain density (g/cc). After pressing, the porosity of the samples ranged from 0.02 to 0.4. They also cored samples from commercially available salt licks (compacted solar evaporated salt). More than 2000 thermal property measurements were taken using guarded heat flow and transient plane source methods. The thermal conductivity of granular salt showed strong temperature dependence: thermal conductivity decreased with increasing temperature and porosity. Specific heat of granular salt increased with increasing temperature, but showed little porosity dependence. They compared their thermal conductivity results to that predicted from the geometric mean of the thermal conductivity of the sample constituents, a mixture model that has been used to estimate thermal conductivity of other geologic materials (Macaulay et al. 2015):

$$K_{gs} = K_0^{1-\phi} K_a^{\phi} \tag{2}$$

where ϕ is porosity, K_{gs} is thermal conductivity of granular salt, K_0 is thermal conductivity of single-crystal halite and K_a is thermal conductivity of air. They found that the measured thermal conductivities were lower than that predicted by Eq. 2 in most cases. Bauer and Urquhart (2015) also measured thermal properties of WIPP salt samples previously deformed in uniaxial compression at elevated temperature (Mellegard et al. 2013) using salt core obtained from the WIPP facility. These samples both flowed and fractured in response to the high temperature (up to 250 °C) and experienced a great amount of axial shortening (20–30%). They found that the small amounts of microcrack porosity (0.02–0.04) created in these dilated samples have a significantly greater effect on the thermal properties than comparable porosities in compressed granular salt. They suggested this result was due to the difference in the pore structure in the two materials: dilated polycrystalline salt tends to develop extensive and well-connected crack/pore networks along grain boundaries, whereas compacted/compressed salt may have more isolated and more equant-shaped pores.

Bechthold et al. (1999, 2004) report thermal properties of granular salt obtained from the Asse facility in Germany. Granular salt obtained during the excavation of test

drifts was sieved to obtain grain sizes less than 45 mm. They compacted granular salt in a triaxial cell without added water at elevated temperatures up to 200 °C and pressures up to 70 MPa. Grain density of salt was determined using a pycnometer, and bulk density was determined from the mass and volume of the salt used in the specimen. Porosity was calculated using Eq. 1. A constant axial strain rate of about 10^{-5} s^{-1} was used for compaction, and volume change was measured by a special pressure/volume control device. Thermal properties of the compacted salt were determined using a transient method in a porosity range of 0.013–0.285. Most of the tests were carried out at room temperature, and a few experiments were carried out at 80 °C. Their initial results suggested a linear relationship between thermal conductivity and porosity (Bechthold et al. 1999):

$$K_{gs} = K_0(1 - 2.7\phi) \tag{3}$$

Similarly, a linear relationship between specific heat of granular salt and porosity was recommended as:

$$C_{gs} = (1 - \phi)C_0 \tag{4}$$

where C_{gs} is specific heat of granular salt and C_0 is the specific heat of single-crystal halite. They reported additional measurements (Bechthold et al. 2004) and indicated a polynomial best fit to data of thermal conductivity and porosity:

$$K_{gs} = K_0(-54\phi^4 + 74\phi^3 - 27.2\phi^2 + 0.3\phi + 1) \tag{5}$$

In this study, measurements of thermal conductivity, specific heat, grain density and porosity are reported for granular salt that has been consolidated under a range of temperature, stress and moisture conditions. The majority of these measurements were taken on samples subjected to hydrostatic creep consolidation with stresses and temperatures relevant to potential repository conditions. Under these conditions, it is likely that the consolidation process generates a pore structure consistent with the deformation mechanisms expected to be operative at repository conditions, particularly with regard to the nature of the grain boundaries. We therefore expect these measurements to be directly relevant to the response of granular salt in a repository application. Thermal conductivity and specific heat measurements on granular salt at different temperature and porosities were fit to various empirical relationships and compared to the results of other workers to determine the validity of these new data and provide a basis for application of these new results to our understandings of the physical nature of porosity (crack, pore and combinations) upon thermal properties. Additional measurements were conducted on a single halite crystal and experimentally deformed dilated polycrystalline salt to complement the measurements taken on granular salt.

2 Materials and Methods

2.1 Sample Material

Thermal property and porosity measurements were taken on four different sample groups: laboratory-consolidated granular salt using two salt types (domal and bedded), granular salt having been consolidated in situ and recovered from an underground research facility in a German domal salt formation, polycrystalline salt cores from the WIPP facility and a single crystal of halite. The granular domal salt was obtained from Avery Island, LA (AI) and the granular bedded salt was obtained from the WIPP facility. The WIPP salt is about 98% halite and contains about including 2% water-insoluble impurities, including quartz, gypsum and clays (Stein 1985). The Avery Island salt is about 99% pure NaCl and is unusually free of anhydrite and clay along grain boundaries and of fluid inclusions and anhydrite crystals within the salt grains (Hansen and Carter 1980).

Thermal property measurements were conducted on 20 samples obtained from these salt types; many of these samples were sub-cored to produce a total of 55 sub-samples used for porosity testing. A summary of samples and sub-samples is given in Table 1.

2.1.1 Laboratory-Consolidated Granular Salt

Mine-run granular salt was obtained from the WIPP facility and the Avery Island salt mine. The granular salt was oven-dried at 105 °C and sieved to obtain particle sizes of less than 9.5 mm. A representative grain size distribution of each salt type is given in Fig. 1. The sieved granular salt was compacted inside a jacket of lead with an inner copper sheath to withstand testing at elevated temperatures. Some specimens had 1% moisture by weight added prior to specimen construction. The resulting cylindrical specimens were 100 mm in diameter, with a nominal height of 200 mm. The initial porosity of the specimens ranged from 0.34 to 0.40.

Specimens were consolidated using hydrostatic stresses up to 38 MPa and temperatures up to 250 °C; this range of conditions encompass plausible stresses and temperatures adjacent to high-level waste. Stresses and strains

Table 1 Samples and sub-samples produced for thermal properties and porosity tests

	Laboratory-consolidated salt		In situ partially consolidated salt	Polycrystalline salt	Halite crystal
	WIPP	AI			
Samples	12	2	3	2	1
Sub-samples	36	8	6	5	

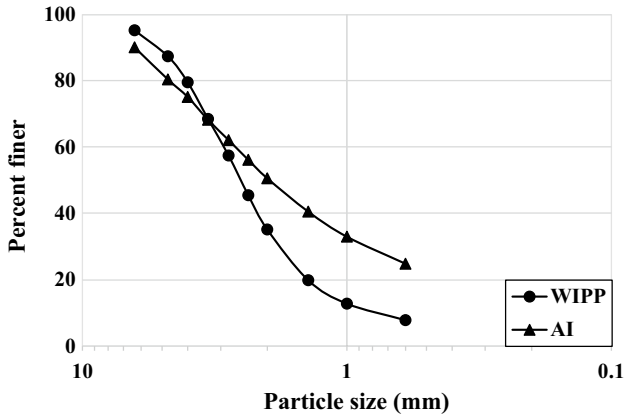

Fig. 1 Typical grain size distribution of granular salt used to produce laboratory-consolidated samples

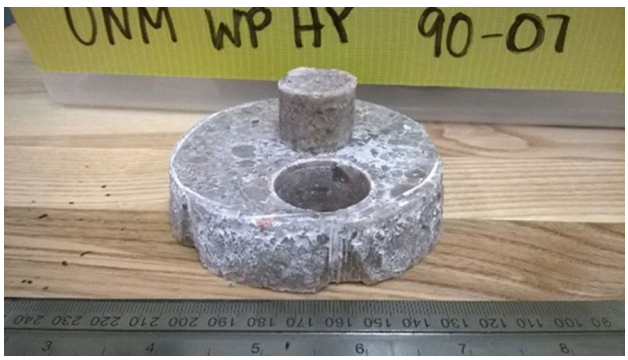

Fig. 2 A 25.4-mm-diameter core obtained from 100-mm-diameter, 25-mm-thick disc of consolidated salt

were derived from measured loads and deformations. Test durations ranged from hours to weeks, and most specimens achieved a final porosity of 0.05 or less. More details regarding the consolidation tests are given by Broome et al. (2014).

After a consolidation test was completed, two discs, each approximately 25 mm thick, were cut from the top and bottom of the consolidated specimen using a diamond wire saw. These discs were used for thermal properties testing. Subsequently, one of the discs was further cored to obtain 25.4- and 38-mm-diameter sub-samples for porosity measurements. These sub-samples were further cut to an approximate height of 12.7 and 25.4 mm (Fig. 2).

2.1.2 In Situ Partially Consolidated Granular Salt

Cores of in situ consolidated granular salt backfill were obtained from an experimental area within the Asse salt mine located in Germany. The backfill was pneumatically stowed in 1985 as part of a heater test initiated in 1990 and terminated in 1999. The backfill had consolidated to a porosity of 0.23 in the heated region and to 0.30 in the non-heated region when cores were obtained and tested in 1999 (Bechthold et al. 1999). In August 2015, additional cores from this backfill were obtained. These samples were obtained from the heated region. The original backfill was placed at a porosity estimated at 35% and has now consolidated to a variable porosity between 20 and 25% (Hansen 2016). The diameter of the cores ranged from 83 to 100 mm. These cores were cut with a wire saw to obtain two discs, each of approximately 25 mm thickness. One of the discs was cored to obtain 25.4-mm-diameter sub-samples. These sub-samples were further cut to an approximate height of 12.7 mm.

2.1.3 Dilated Polycrystalline Salt

Two 100-mm-diameter cylindrical cores of polycrystalline salt obtained from the WIPP facility were subjected to uniaxial compression testing: one at 200 °C and one at 250 °C; the salt was deformed by a combination of intracrystalline plasticity and microfracturing which caused dilation (Mellegard et al. 2013). The cores were subsequently cut along their vertical axis, and thermal properties were determined at four different locations on the planar cut by Bauer and Urquhart (2015). They quantified microcrack density at those locations in terms of linear crack density by counting the number of cracks encountered per unit length of traverse across the sample. Crack aperture was not measured. For this study, one of the cut halves was further cut along the horizontal and vertical axes to measure thermal conductivity in both the planes. Also, 25.4-mm-diameter sub-samples with heights of 12.7 and 25.4 mm were obtained to determine porosity.

2.1.4 Halite Crystal

A halite crystal of optically clear halite was obtained from the Hockley Salt Dome in Texas. The crystal had a width of 75 mm and a height of 50 mm (Urquhart and Bauer 2015). The crystal was assumed to have zero porosity.

2.2 Methods

2.2.1 Porosity Measurements

Porosity measurements were taken on sub-samples using a helium gas expansion porosimeter (Anovitz and Cole 2015; Coberly and Stevens 1933) to measure gas-accessible or effective porosity. In addition, total porosity measurements were taken based on the sample's measured mass and volume (referred to as the MV method) and an assumed grain density of 2.16 g/cc (Yang 1981; Birch and Clark 1940) and utilized Eq. 1 to calculate porosity. Based on independently measuring a sub-sample dimensions 23 times, the standard deviation in the calculated porosity was 0.002.

In addition to the porosity measured on sub-samples described above, the porosity of the central core from consolidated specimens was measured in a differential pressure permeameter that served as a gas expansion porosimeter. During the conduct of permeability tests on the central core, an initial pore pressure in the sample was established by introducing gas to the sample from a reservoir of known volume and pressure. The subsequent equilibrium pressure under isothermal conditions was used to estimate the connected pore volume in the sample. The porosity was calculated from Eq. 1 using the measured dimensions of central core and an assumed grain density of 2.16 g/cc.

2.2.2 Thermal Properties Measurement

Thermal properties measurements were taken using the transient plane source method (Bahrami et al. 2016) with a Hot Disk® TPS 1500. For this method, a heat pulse was applied with a thin plane sensor that was sandwiched between two pieces of consolidated salt. Thermal properties were interpreted numerically from the dissipation of the heat pulse with time.

Two discs of salt with a diameter and thickness greater than the radius of the sensor were used, as recommended by the manufacturer. These discs were polished on one side to get a smooth and clean surface using fine sand paper and isopropanol. The thermal sensor was then pressed between the two polished sides and modest pressure was applied across the discs using a screw clamp (Fig. 3). During a measurement, a heat pulse was supplied by the sensor and the transient temperature response was recorded for 20–40 s. A computer program integrated into the measurement system solved the transient heat equation for the thermal properties that best fit the measured temperature response. This solution assumes the thermal properties are uniform throughout the sample and thus averages out any local porosity and grain size heterogeneities (Bauer and Urquhart 2015). Heat energy was dissipated by waiting 20 min between measurements. Typically, three to five sets of measurements at each temperature were made at the same location and averaged; eachset of measurements consisted of 5 individual measurements. Thus, each reported value represents an average of 15–25 individual measurements. Measurements were taken at temperatures up to the maximum temperature experienced during the consolidation testing or the uniaxial compression testing in the case of the dilated polycrystalline salt tests. In situ consolidated samples were tested up to 150 °C.

Thermal tests were repeated on a consolidated salt sample 10 separate times to evaluate repeatability of the measurement. In each test, the sample was removed from test device and the sensor was repositioned in a different location before the next test was conducted. The standard deviation in thermal conductivity and specific heat at 50 °C estimated from the repeated measurements were 0.237 W/mK and 0.114 MJ/m^{3}K, respectively.

2.2.3 Microscopic Observations

Observations were completed upon thin sections made from hydrostatically consolidated salt samples and some pellet compressed samples from the tests of Bauer and Urquhart (2015) with comparable densities. Hydrostatically consolidated samples were vacuum-impregnated with low-viscosity epoxy that was doped with rhodamine-B dye and cut with an Isomet® saw on a thin section chuck. The cut pieces were polished with a 1200 grit sandpaper until they had 1 mm thickness. A Leitz Ortholux II optical microscope equipped with a Leica camera and Leica Application Suite software was used for microscopic observations. The pellet samples' thin sections were commercially prepared in a similar manner. Photomicrographs of both the salt types were taken at 5× magnification of the objective.

3 Results and Discussion

3.1 Porosity

Porosity and grain density of all salt types are summarized in Table 2. Porosity of sub-samples ranged between 0.005

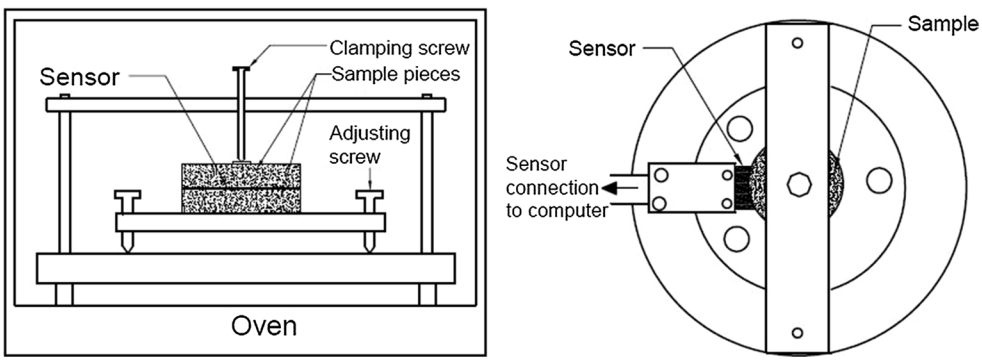

Fig. 3 Schematic of thermal properties test arrangement shown in plan (right) and elevation (left)

Table 2 Summary of porosity test results obtained from various methods and grain density measured using porosimeter

Types of salt	Sample ID[a]	Laboratory consolidation		Porosimeter grain density (g/cc)	Sub-sample porosity		Porosity of central core
		Temperature (°C)	Stress (MPa)		Porosimeter	MV	
Laboratory-consolidated salt	W-01	90	20	2.158	0.122	0.123	0.048
	W-02*	90	20	2.160	0.035	0.036	0.015
	W-03*	90	20	2.171	0.221	0.217	
	W-04*	90	20	2.163	0.043	0.042	0.030
	W-05*	90	20	2.163	0.019	0.017	0.014
	W-06	90	40	2.158	0.057	0.058	0.019
	W-07	90	38	2.170	0.328	0.253	
	W-08	175	38	2.150	0.062	0.066	0.047
	W-09	175	20	2.157	0.049	0.050	0.023
	W-10	175	20	2.164	0.045	0.043	0.022
	W-11	250	20	2.142	0.005	0.014	0.012
	W-12	250	20	2.167	0.018	0.014	
	A-01	250	20	2.164	0.027	0.025	
	A-02*	250	20	2.161	0.012	0.011	
Polycrystalline salt[b]	D-01	200	N/A	2.161	0.022	0.021	
	D-02	250	N/A	2.181	0.032	0.026	
In situ consolidated salt[c]	B-1-01	N/A	N/A	2.192	0.252	0.249	
	B-1-02	N/A	N/A	2.181	0.209	0.211	
	B-2-01	N/A	N/A	2.191	0.262	0.260	

*Samples with 1% additional moisture added prior to consolidation

[a]The letters indicate the source of the salt: W and A are granular salt from WIPP and Avery Island, respectively; D is from core obtained from WIPP facility; and B is from Asse facility. For B samples, first number designates which core sample came from, additional numbers identify individual sample number

[b]D samples were cored from the WIPP facility and tested for uniaxial compressive strength at the temperatures indicated (Mellegard et al. 2013)

[c]Consolidation conditions as per Bechthold et al. (1999)

and 0.328. The average grain density of granular salt using WIPP and AI salt obtained from the porosimeter method performed on 58 unique measurements was 2.161 g/cc with a standard deviation of ± 0.009 g/cc. Grain density of Asse samples determined from the porosimeter was comparatively greater than the other salt types; however, this value is consistent with the value of 2.187 g/cc reported by Bechthold et al. (1999) for salt from the Asse facility.

Porosity of laboratory-consolidated samples determined from the porosimeter and MV methods was very close to one another (Fig. 4a). Similarly, the porosity of dilated and Asse salt samples obtained using these methods was almost equal. In a few instances, porosity from the MV method yielded slightly lower values than porosity from the porosimeter; this result may be a consequence of the assumed grain density used in the MV method being different than the grain density of that particular sample. The similarity of porosities calculated using the porosimeter, which determines connected porosity, and the MV method, which estimates total porosity, indicated that the porosity of laboratory-consolidated samples was largely connected even for samples consolidated to a porosity of 0.02. This implies that consolidated salt with a porosity of 0.02 would have a measurable permeability. This result is important because others have estimated that reconsolidated rock salt should approach extremely low permeabilities comparable to intact rock salt at porosities of 0.05 (Spiers and Brzesowsky 1993). Porosity of sub-samples measured with the porosimeter was greater than the porosity of central cores measured using the permeameter, i.e. the porosity of sample ends is greater than that of the central core (Fig. 4b). This is consistent with the observation that after consolidation, the specimen had a slightly hourglass shape with the central portion smaller than that near the end pieces.

To investigate the porosity variability within a parent sample of laboratory-consolidated salt, two discs were cored to produce 5 sub-samples each. The sub-samples were cored approximately equidistant from centre to centre of the individual cores and the centre of the disc for maximum utilization of the material (Fig. 5). All values fall within ± 0.005 of the mean porosity values.

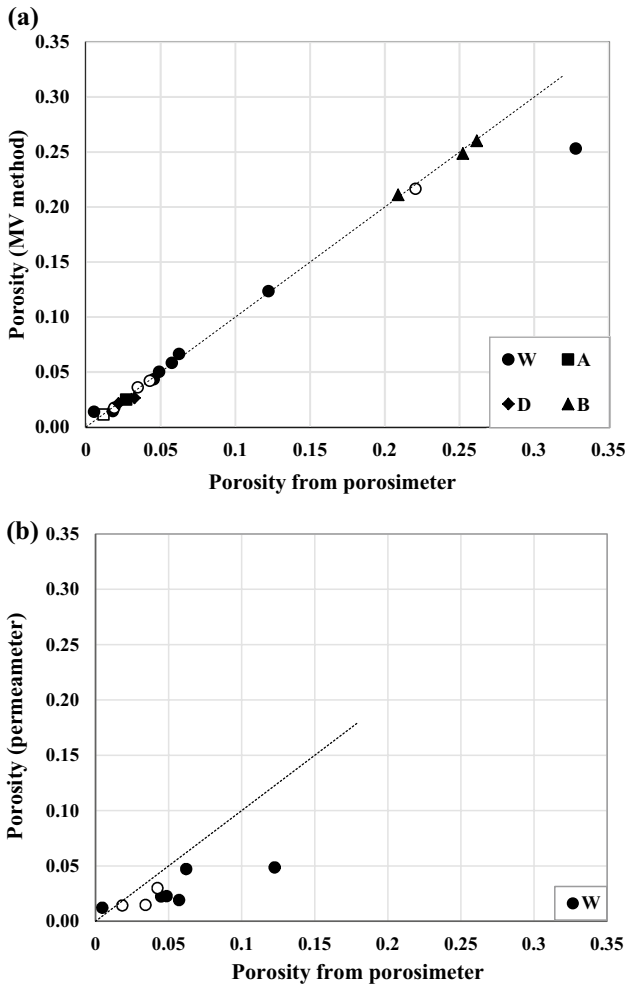

Fig. 4 Comparison of porosities obtained from **a** porosimeter method and MV method and **b** porosimeter method and permeameter method. Open symbols are for samples with 1% additional moisture added prior to consolidation

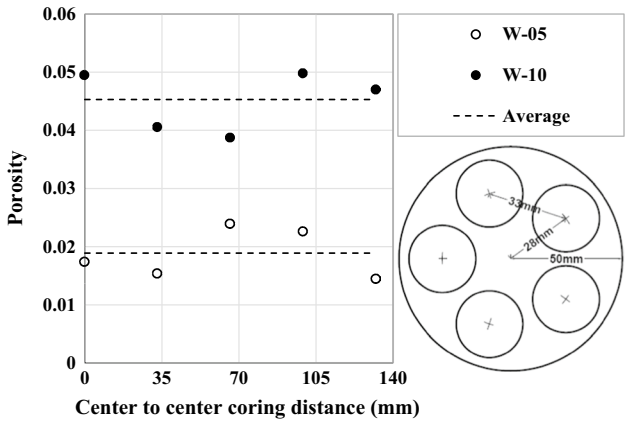

Fig. 5 Radial variability of porosity in laboratory-consolidated samples. The location of sub-samples obtained from each disc is shown in plan view at lower right

3.2 Thermal Properties

Thermal conductivity and specific heat of a halite crystal, laboratory-consolidated salt, dilated salt and in situ consolidated salt at various temperatures are given in Table 3 and plotted versus porosity in Fig. 6.

3.2.1 Halite Crystal

Results indicate that thermal conductivity of the halite crystal decreases with increase in temperature, which is consistent with the results of others (Bechthold et al. 1999; Durham and Abey 1981; Birch and Clark 1940; Smith 1976; Acton 1977; Sweet and McCreight 1979; Urquhart and Bauer 2015; Yang 1981). Specific heat of the halite crystal increases with increase in temperature, which is consistent with results by others (Bechthold et al. 1999; Smith 1976; Yang 1981). In contrast, Urquhart and Bauer (2015) found no clear temperature dependence of specific heat for a single crystal of halite.

3.2.2 Granular Salt

Granular salt experimental results show that thermal conductivity decreases with increase in temperature and porosity, consistent with results from Bechthold et al. (1999) and Bauer and Urquhart (2015). Specific heat of granular salt increases with increase in temperature at lower porosities. At higher porosities, temperature dependence is not apparent. At lower temperatures, specific heat decreases with increase in porosity. At higher temperatures, porosity dependence is not apparent. Bauer and Urquhart (2015) reported specific heat of granular salt showed little porosity dependence but increased with increase in temperature. Bechthold et al. (1999) reported specific heat decreased with an increase in porosity at room temperature.

Thermal conductivities from this study were generally greater than those measured by Bauer and Urquhart (2015) at all temperatures (Fig. 7). Both studies used largely the same granular salt source and the same measurement methods, but employed different sample preparation methods. Bauer and Urquhart (2015) rapidly pressed granular salt into pellets at room temperature, whereas this study involved hydrostatic consolidation of granular salt at elevated temperatures and pressures and for much longer durations.

Microscopic observations were conducted to investigate the differences in thermal conductivities between consolidated and pressed samples. Photomicrographs of hydrostatically consolidated and pressed samples with similar porosities of about 0.02 are shown in Fig. 8. The hydrostatically consolidated sample has fully sutured or fused grain boundaries and a near absence of microcracks. The consolidation involved gradual (quasi-static) hydrostatic pressure loading and unloading at elevated temperature. This testing

Table 3 Thermal properties of various salt types measured in a range of 50 °C to 250 °C

Types of salt	Sample	Thermal conductivity (W/mK)					Specific heat (MJ/m^{3}K)				
		50 °C	100 °C	150 °C	200 °C	250 °C	50 °C	100 °C	150 °C	200 °C	250 °C
Laboratory-consolidated salt	W-01	4.30					2.15				
	W-02*	5.44					1.20				
	W-03*	2.70					1.99				
	W-04*	4.81					2.02				
	W-05*	5.09					1.74				
	W-06	4.75					1.70				
	W-07	1.85					0.56				
	W-08	4.10	3.37	2.87			1.91	1.87	1.88		
	W-09	4.38	4.07	3.78			1.85	2.04	2.19		
	W-10	4.40	4.08	3.74			2.03	2.18	2.33		
	W-11	5.02	4.73	4.32	3.86	3.53	1.97	2.21	2.42	2.47	2.62
	W-12	5.19	4.72	4.31	3.84	3.50	2.01	2.21	2.46	2.61	2.70
	A-01	5.38	4.94	4.54	4.13	3.76	1.96	2.17	2.39	2.53	2.64
	A-02*	5.45	5.11	4.67	4.28	3.89	2.07	2.21	2.39	2.52	2.58
Dilated salt	D-01	4.06	3.81	3.48	3.28		1.94	2.06	2.31	2.37	
	D-02	4.22	3.91	3.63	3.39		1.74	1.994	2.225	2.4	
In situ consolidated salt	B-1-01	2.15	1.97	1.61			1.27	1.42	1.37		
	B-1-02	2.48	2.25	1.83			1.41	1.53	1.45		
	B-2-01	2.20	2.01	1.68			1.06	1.27	1.26		
Halite crystal	SC-01	5.55	5.05	4.56	4.31	3.92	2.06	2.15	2.38	2.48	2.63

*Samples with 1% additional moisture added prior to consolidation

procedure is expected to promote plastic deformation during consolidation and prevent cracking during unloading (depressurization). Grain boundaries coalesced by plastic deformation at a molecular scale. The presence of water favours consolidation (Stormont and Finley 1996), whether as added or mobilized from the salt at elevated temperatures (Broome et al. 2014). As consolidation proceeds, the porosity will consist of a network of smaller and smaller pores between regions of healed or fused grain boundaries. In contrast, the pressed samples experienced relatively rapid loading to high stresses and unloading (minutes) at ambient temperature. This type of loading resulted in cleavage cracking and microfracturing at grain boundaries. At high porosities, cracks formed at grain contacts during mechanical consolidation. As the pressing progressed, most of the porosity subsequently closed. Upon unloading, however, the stored strain energy within the grains is relieved by the formation of cracks along grain boundaries and through grains along cleavage planes, and is made apparent by the presence of stained epoxy.

Differences in heat flow through consolidated salt and pressed salt can be explained by the differences in the nature of their porosity. Conduction finds a preferred path through the solid matrix of salt, which is more than 100 times more conductive than the air (Joy 1957). Hence heat flow is expected to readily circumvent the pore network that develops in consolidated salt, whereas it must cross open grain boundaries and microcracks in samples with crack porosity such as pressed salt. Heat flow is inhibited more in the latter case and results in a lower thermal conductivity at a comparable density.

Applying the mixing law (Macaulay et al. 2015) (Eq. 2), 1% added water would increase the thermal conductivity by more than 5% which is within the resolution of the measurement technique. However, the samples consolidated with 1% added water do not result in systematically greater thermal conductivities compared to samples compacted without added water (Table 3 and Fig. 6). The added water was likely involved in pressure solutioning at grain contacts (Spiers and Brzesowsky 1993), which involves the dissolution and precipitation of salt at grain boundary contacts. This mechanism may produce isolated fluid inclusions along remnant grain boundaries and not a continuous water phase within a pore network; isolated pores and fluid inclusions may not significantly impact the effective thermal properties for the entire mass. Further, at the elevated temperatures during the consolidation test, some of the added water may have evaporated and been removed from the vented samples.

There were only two tests on AI salt; both samples were consolidated at 250 °C. Compared to the WIPP salt, the

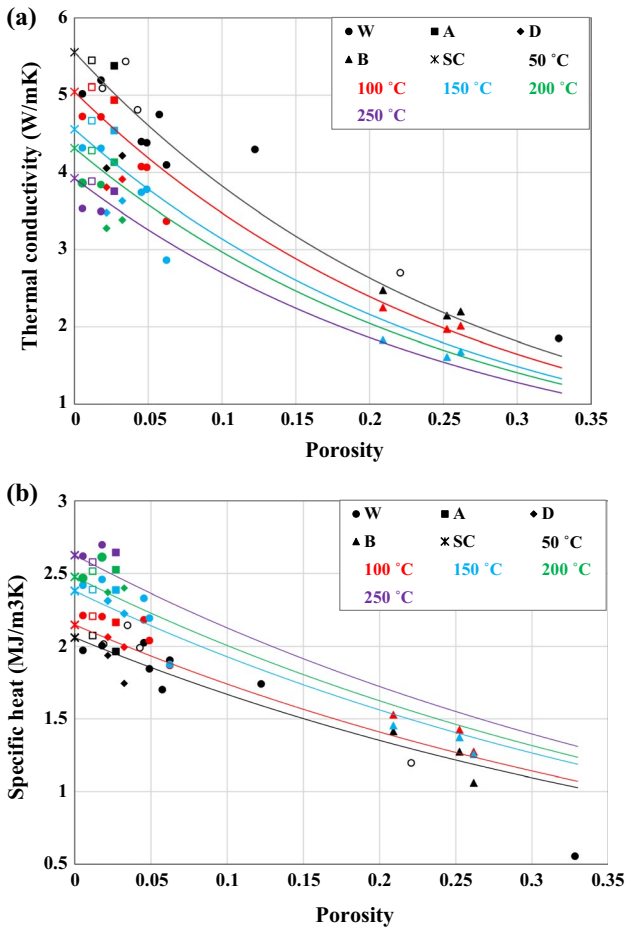

Fig. 6 Thermal conductivity (**a**) and specific heat (**b**) of samples as a function of porosity at various temperatures. Colours indicate temperature at which thermal properties were measured. Symbol shapes designate source of salt. Open symbols are for samples with 1% additional moisture added prior to consolidation. Lines represent exponential fits to thermal properties

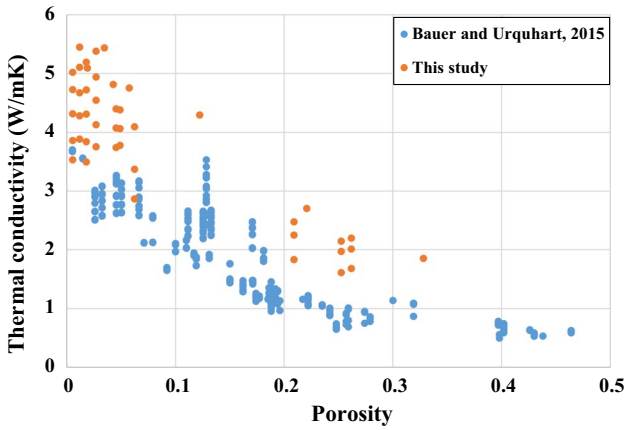

Fig. 7 Thermal conductivity of consolidated salt compared with pellet pressed salt (from Bauer and Urquhart 2015) in a temperature range of 50–250 °C

thermal conductivity of AI salt is greater at comparable porosities and at higher temperatures (Table 3 and Fig. 6). Differences in thermal conductivity may be a result of differing amounts of impurities (Clauser and Huenges 1995) in the two types of salt; WIPP salt has between 1 and 5% water-insoluble impurities (Stein 1985), whereas the AI salt has roughly 0.7% of water-insoluble impurities (Durham and Abey 1981). At comparable porosities, there is little difference in the specific heat of WIPP and AI salt.

3.2.3 Dilated Salt

Thermal conductivities of the dilated salt samples are given in Fig. 9. For each sample, separate measurements were taken in the vertical and horizontal planes. For sample D-01, the vertical and horizontal thermal conductivity values nearly coincide, whereas in the other sample the values along the horizontal plane are larger. In all cases, the thermal conductivity decreased with increasing temperature.

The dilated polycrystalline salt had a lower thermal conductivity compared to consolidated salt at a comparable porosity (Fig. 6a). The porosity of dilated salt consists of a network of high-aspect ratio microcracks (width to height) along grain boundaries (Stormont and Daemen 1992), whereas in consolidating granular salt, the porosity evolves towards a network of pores adjacent to fused grain boundaries (Hansen et al. 2014). Heat flow will likely be more inhibited by the pervasive crack network as suggested by Bauer and Urquhart (2015). The microcracks formed in uniaxial compression should be preferentially aligned vertically along the core axis, and therefore, we expect the thermal conductivity measured on a vertical plane would be lower than that measured on the horizontal plane. However, our results did not reveal a clear trend between the thermal conductivity measured on different planes and the assumed microcrack orientation.

3.3 Thermal Properties Models

Measured thermal conductivity and specific heat of a halite crystal were fit as a function of temperature to linear, quadratic, cubic and exponential expressions and were also fit to models from other studies on single-crystal halite (Table 4). Sum of the squared errors (SSE) were calculated using measured and predicted values of thermal conductivity (K) and specific heat (C) using Eqs. 6 and 7.

$$\mathrm{SSE} = \Sigma\left(K_{\mathrm{measured}} - K_{\mathrm{predicted}}\right)^2 \tag{6}$$

$$\mathrm{SSE} = \Sigma\left(C_{\mathrm{measured}} - C_{\mathrm{predicted}}\right)^2 \tag{7}$$

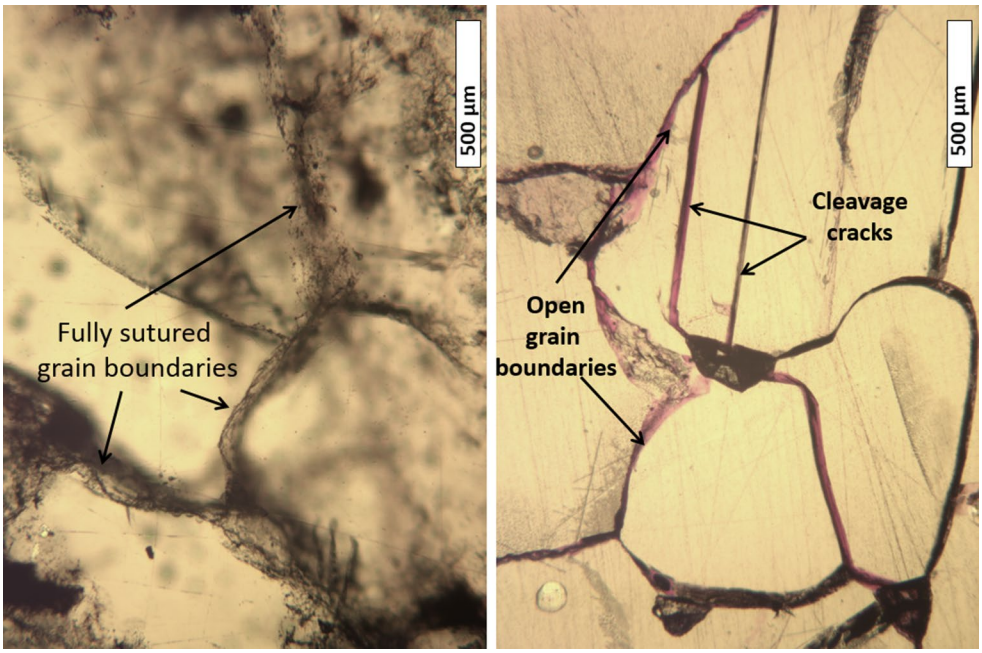

Fig. 8 Consolidated salt (left) and axially pressed salt (right) at comparable porosities of less than 0.02

Higher-order polynomials provide a slightly better fit but are more likely to significantly deviate from expected trends if used to extrapolate beyond the measured data. Expressing thermal properties as a linear function of temperature is a common form for other geologic minerals (Clauser and Huenges 1995) and has previously been used for rock salt (Bechthold et al. 1999; Clark Jr 1969). For a data set from a larger range of temperatures, a higher-order polynomial fit may be more appropriate, such as that given by Urquhart and Bauer (2015) for a range from − 75 to 300 °C. Of existing models for single-crystal halite properties, our data were best fit to the polynomial expressions of Yang (1981).

Thermal properties of granular salt were fit to the following expressions

$$K_{gs}(T,\phi) = K_0(T)f(\phi) \tag{8}$$

$$C_{gs}(T,\phi) = C_0(T)g(\phi) \tag{9}$$

With these expressions, the dependence on temperature is accounted by the term for the thermal property of the halite crystal. The second term in these expressions is a function of porosity only. Using the linear expressions for thermal conductivity and specific heat given in Table 4 for $K_0(T)$ and $C_0(T)$, various forms for the functional dependence on porosity ($f(\phi)$ and $g(\phi)$) were fit to data (Table 5) and also fit to expressions from other studies on granular salt. Quadratic, cubic and exponential forms perform nearly equally; the exponential form is used to model thermal conductivity and specific heat in Fig. 6a, b, respectively. Of existing models for granular salt thermal properties, our data were best fit to the linear model of Bechthold et al. (1999).

4 Conclusions

The similarity of porosities derived from porosimeter, which determined connected porosity, and MV method, which estimated the total porosity, indicates that the porosity of laboratory-consolidated samples is largely connected even to porosities as low as 2%. This result is in contrast to others that have estimated that pore networks in consolidating granular salt become largely disconnected at around 5% porosity (Spiers and Brzesowsky 1993; Holcomb and Shields 1987). Porosity of sub-samples obtained from the ends of the cores was mostly greater than that from the central portion of the cores. This result suggests that the specimens did not deform uniformly.

Thermal conductivity of a single crystal of halite showed strong dependence on temperature, i.e. thermal conductivity decreased with increase in temperature. These data were well fit as a linear function of temperature which is a common form for other geologic minerals. Thermal conductivity of granular salt was dependent on temperature and porosity;

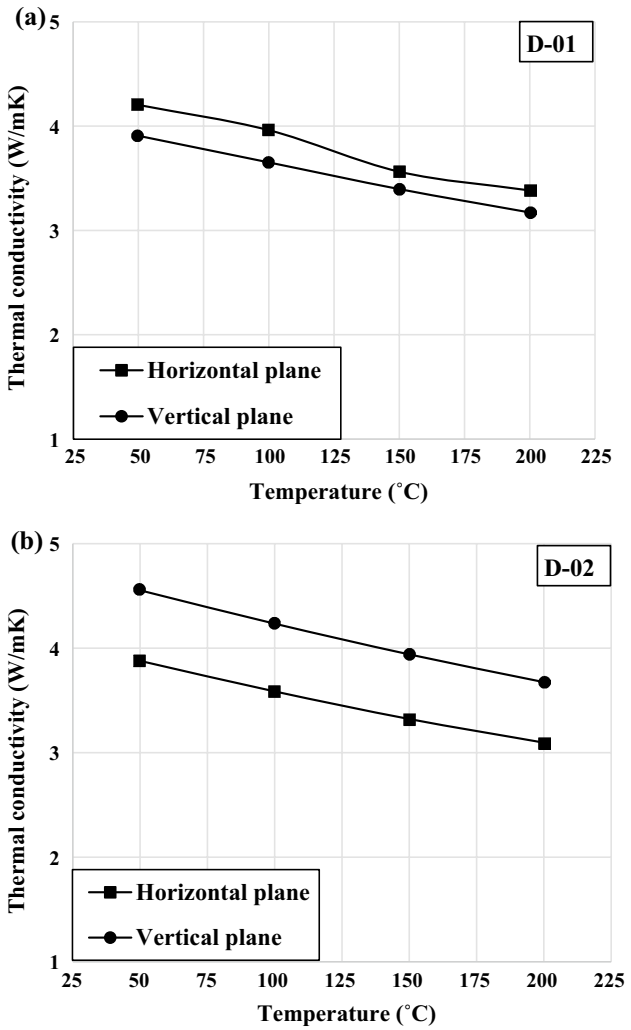

Fig. 9 Thermal conductivity of dilated polycrystalline salt: D-01 (**a**) and D-02 (**b**)

thermal conductivity decreased with an increase in temperature and porosity. There was no significant difference in thermal conductivity for samples consolidated with 1% added moisture and those without added moisture at comparable porosities. At a comparable porosity, domal salt (AI) has a greater thermal conductivity than bedded salt (WIPP) at all temperatures. This is possibly due to varying proportion of water-insoluble impurities in these salt types. Thermal conductivity of granular salt was expressed as a function of the thermal conductivity of single-crystal halite and the porosity, as $K_{gs}(T,\phi) = K_0(T)f(\phi)$. Quadratic, cubic, quartic and exponential forms for $f(\phi)$ were found to perform nearly equally well in capturing the dependence on porosity.

Specific heat of a single crystal of halite was shown to increase with an increase in temperature, which was fit with a linear function. Specific heat of granular salt at lower temperatures was shown to decrease with an increase in porosity. At higher temperatures, porosity dependence was not apparent. The specific heat of granular salt was expressed as a function of the specific heat of single-crystal halitel and the porosity, $C_{gs}(T,\phi) = C_0(T)g(\phi)$. Quadratic, cubic, quartic and exponential forms for $g(\phi)$ were found to perform nearly equally well in capturing the dependence on porosity; however, additional measurements would be useful to confirm the trends implied from the data and verify the model fits. There was no significant difference in specific heat for samples consolidated with 1% added moisture and those without added moisture at comparable porosities.

Thermal conductivities measured in this study were generally greater than that those measured by Bauer and Urquhart (2015) at all temperatures in spite the fact that the granular salt stock material was largely from the same location (WIPP) and the same measurement method was used. Bauer and Urquhart (2015) pressed granular salt in pellets at room temperature, whereas this study involved hydrostatic consolidation of granular salt at elevated temperatures and pressures. Photomicrographs of hydrostatically consolidated and pressed samples with the same porosities showed that the hydrostatically consolidated sample had fully sutured grain boundaries and a near absence of microcracks. In contrast, the pressed samples had intense cleavage cracks and microfracturing at grain boundaries.

Thermal conductivity of dilated salt was determined to be lower than the consolidated salt at comparable porosities. The pervasive crack network along grain boundaries in dilated salt limits heat flow and results in a lower thermal conductivity compared to hydrostatically consolidated salt. The measurements on both the dilated salt and pressed salt samples demonstrate the dramatic effect of cracks upon thermal conductivity andthus heat transfer. The implication in a repository setting where micro- and macrofractures may form during the room closure process is that the presence of fractures may inhibit heat flow.

The majority of the thermal and porosity measurements were taken on samples subjected to hydrostatic creep consolidation with stresses and temperatures relevant to potential repository conditions. Creep consolidation tests generated a pore structure consistent with the deformation mechanisms expected to be operative at repository conditions, particularly with regard to the nature of the grain boundaries. We therefore expect these measurements to be directly relevant to the response of granular salt in a repository application. The empirical models derived from these measurements can be used in thermomechanical models of repository behaviour.

Table 4 Thermal properties of a halite crystal fitted to empirical equations and compared to other models

		SSE
Thermal conductivity equations		
Fitting to simple expressions	$K_0 = -7.98 \times 10^{-3}T + 5.876$	0.025
	$K_0 = 1.374 \times 10^{-5}T^2 - 1.21 \times 10^{-2}T + 6.116$	0.008
	$K_0 = -1.12 \times 10^{-7}T^3 + 6.414 \times 10^{-5}T^2 - 1.87 \times 10^{-2}T + 6.352$	0.005
	$K_0 = 5.996e^{-0.002T}$	0.218
Comparison to other models	$K_0 = 1.2 \times 10^{-1}T^{-2} - 6.11T + 7.01$ (Smith 1976)	1.210
	$K_0 = -1.717 \times 10^{-8}T^3 + 3.12 \times 10^{-5}T^2 - 2.1 \times 10^{-2}T + 7.07$ (Yang 1981)	0.646[a]
	$K_0 = -1.51 \times 10^{-8}T^3 + 2.86 \times 10^{-5}T^2 - 1.838 \times 10^{-2}T + 5.734$ (Bechthold et al. 1999)	5.237
	$K_0 = -2 \times 10^{-7}T^3 + 1 \times 10^{-4}T^2 - 3.17 \times 10^{-2}T + 6.8203$ (Urquhart and Bauer 2015)	6.887
Specific heat equations		
Fitting to simple expressions	$C_0 = 2.92 \times 10^{-3}T + 1.9$	0.004
	$C_0 = -3.43 \times 10^{-7}T^2 + 3.02 \times 10^{-3}T + 1.894$	0.004
	$C_0 = -6 \times 10^{-8}T^3 + 2.665 \times 10^{-5}T^2 - 5.17 \times 10^{-4}T + 2.02$	0.005
	$C_0 = 1.929e^{0.0013T}$	0.006
Comparison to other models	$C_0 = -1.09 \times 10^{-3}T^{-2} + 2.83 \times 10^{-2}T + 2.06 \times 10^{-1}$ (Smith 1976)	1.048
	$C_0 = 3.499 \times 10^{-10}T^3 - 8.453 \times 10^{-7}T^2 + 6.43 \times 10^{-4}T + 1.864$ (Yang 1981)	0.210[a]
	$C_0 = 0.177T + 855$ (Bechthold et al. 1999)	1.010

[a]Thermal conductivity and specific heat equations were obtained by fitting the recommended values. T is temperature in Celsius except for equations suggested by Smith (1976) are in Kelvin

Table 5 Thermal properties of granular salt fitted to empirical equations and other models

		SSE
Thermal conductivity equations		
Fitting to simple expressions	$K_{gs} = K_0(1 - 2.46\phi)$	5.869
	$K_{gs} = K_0(5.08\phi^2 - 3.696\phi + 1)$	4.140
	$K_{gs} = K_0(-1.207\phi^3 + 5.556\phi^2 - 3.735\phi + 1)$	4.138
	$K_{gs} = K_0(47.64\phi^4 - 29.44\phi^3 + 10.23\phi^2 - 3.89\phi + 1)$	4.111
	$K_{gs} = K\, e^{-3.73\phi}$	4.168
Comparison to other models	$K_{gs} = K_0(1 - 2.7\phi)$ (Bechthold et al. 1999)	7.214
	$K_{gs} = K_0(-54\varphi^4 + 74\varphi^3 - 27.2\varphi^2 + 0.3\varphi + 1)$ (Bechthold et al. 2004)	13.360
	$K_{gs} = K_0^{1-\phi}K_a^{\phi}$ (Macaulay et al. 2015)	10.464
Specific heat equations		
Fitting to simple expressions	$C_{gs} = C_0(1 - 1.7\phi)$	0.655
	$C_{gs} = C_0(-2.525\phi^2 - 1.17\phi + 1)$	0.535
	$C_{gs} = C_0(-8.305\phi^3 - 0.5\phi^2 - 1.04\phi + 1)$	0.477
	$C_{gs} = C_0(-383.77\phi^4 + 221.75\phi^3 - 39.61\phi^2 + 0.43\phi + 1)$	0.372
	$C_{gs} = C_0\, e^{-2.107\phi}$	0.850
Comparison to other models	$C_{gs} = C_0(1 - \phi)$ (Bechthold et al. 1999)	2.257
	$C_{gs} = C_0(1 - \phi) + C_a\phi$ (Jury and Horton 2004)	2.259

T is temperature in Celsius and ϕ is porosity

Acknowledgements Funding was provided through the Department of Energy's Nuclear Energy University Program (Grant DE-NE0000733). Sandia National Laboratories is a multi-programme laboratory managed and operated by Sandia Corporation, a wholly owned subsidiary of Lockheed Martin Corporation, for the US Department of Energy's National Nuclear Security Administration under Contract DE-AC04-94AL85000.

References

Acton U (1977) Thermal conductivity of S.E. New Mexico Rocksalt and Anhydrites. In: International conference on thermal conductivity, Ottawa, pp 263–276

Anovitz LM, Cole DR (2015) Characterization and analysis of porosity and pore structures. Rev Miner Geochem 80:61–164

Bahrami M, Ahadi M, Andisheh-Tadbir M, Tam M (2016) An improved transient plane source method for measuring thermal conductivity of thin films: deconvoluting thermal contact resistance. Int J Heat Mass Transf 96:371–380. https://doi.org/10.1016/j.ijheatmasstransfer.2016.01.037

Bauer S, Urquhart A (2015) Thermal and physical properties of reconsolidated crushed rock salt as a function of porosity and temperature. Acta Geotech. https://doi.org/10.1007/s11440-015-0414-8

Beauheim RL, Roberts RM (2002) Hydrology and hydraulic properties of a bedded evaporite formation. J Hydrol 259:66–88

Bechthold W, Rothfuchs T, Poley A, Ghoreychi M, Heusermann S, Gens A, Olivella S (1999) Backfilling and sealing of underground repositories for radioactive waste in salt (Bambus Project): Final Report. EUR 19124 EN. European Commission, Brussels

Bechthold W, Smailos E, Heusermann S, Bollingerfehr W, Bazargan Sabet B, Rothfuchs T, Kamlot P, Grupa J, Olivella S, Hansen F (2004) Backfilling and sealing of underground repositories for radioactive waste in salt (Bambus II Project): Final Report. EUR 20621 EN. European Commission, Luxembourg

Birch F, Clark H (1940) The thermal conductivity of rock and its dependence upon temperature and composition: part I. Am J Sci 238:529–558

Broome ST, Bauer SJ, Hansen FD (2014) Reconsolidation of crushed salt to 250 °C under hydrostatic and shear stress conditions. In: 48th US rock mechanics/geomechanics symposium, Minneapolis

Carter N, Hansen FD (1983) Creep of rocksalt. Tectonophysics 92:275–333

Clark Jr SP (1969) Heat conductivity in the mantle. In: Hart PJ (ed) The earth's crust and upper mantle. American Geophysical Union Geophysical Monograph vol 13. Washington, pp 622–626

Clauser C, Huenges E (1995) Thermal conductivity of rocks and minerals. In: A handbook of physical constants. AGU Reference Shelf 3. American Geophysical Union, pp 105–125

Coberly CJ, Stevens AB (1933) Development of hydrogen porosimeter. Society of Petroleum Engineers. SPE-933261-G, pp 261–269

Conca J, Sage S, Wright J (2005) Nuclear energy and waste disposal in the age of fuel recycling. N M J Sci 45:13–21

Cosenza P, Ghoreychia M, Bazargan-Sabeta B, de Marsily G (1999) In situ rock salt permeability measurement for long term safety assessment of storage. Int J Rock Mech Min Sci Geomech Abstr 36:509–526

Damveld H, Bannink D (2012) Management of spent fuel and radioactive waste. State of affairs, a worldwide overview. Nucl Monit 746/7/8

Durham WB, Abey AE (1981) Thermal properties of Avery Island salt to 573 K and 50-MPa confining pressure. Lawrence Livermore National Laboratory, Livermore. UCRL-53128

Hansen FD (2016) Characterization of reconsolidated crushed salt from the BAMBUS Site. SAND2016-2794. Sandia National Laboratories, Albuquerque

Hansen FD, Carter NL (1980) Creep of rock salt at elevated temperature. In: Summers DA (ed) Proceedings of 21st U.S. symposium on rock mechanics. University of Missouri, Rolla, pp217–226

Hansen F, Popp T, Wieczorek K, Stuhrenberg D (2014) Granular salt summary: reconsolidation principles and applications. SAND2014-16141R. Sandia National Laboratories, Albuquerque

Holcomb DJ, Shields M (1987) Hydrostatic creep consolidation of crushed salt with added water. SAND87-1990. Sandia National Laboratories, Albuquerque

Joy AF (1957) Thermal conductivity of insulation containing moisture. ASTM International, West Conshohocken, pp 65–67

Jury WA, Horton R (2004) Soil physics, 6th edn. Wiley, Hoboken, pp 180–182

Macaulay DB, Bouazza A, Wang B, Singh RM (2015) Evaluation of thermal conductivity of models. Can Geotech J 52:1892–1900

Martin BL, Rutqvist J, Birkholzer JT (2015) Long-term modeling of the thermal-hydraulic-mechanical response of a generic salt repository for heat-generating nuclear waste. Eng Geol 193:198–211. https://doi.org/10.1016/j.enggeo.2015.04.014

Mellegard K, Callahan G, Hansen F (2013) High-temperature characterization of bedded Permian salt. 47th US rock mechanics/geomechanics symposium

National Research Council (2001) Disposition of high level waste and spent nuclear fuel. Committee on Disposition of High Level Radioactive Waste through Geological Isolation. Board of Radioactive Waste Management, pp 22–26. ISBN: 0-309-56764-5

Smith D (1976) Thermal conductivity of halite using a pulsed laser. Report no.: Y/DA-7013. Oak Ridge (TN): Oak Ridge Y- Plant; 1976. Contract no.: W- 7405-eng-26. Supported by the US Energy Research and Development Administration

Spiers CJ, Brzesowsky RH (1993) Densification behavior of wet granular salt: theory versus experiment. Seventh symposium on salt, 1993. vol I. Elsevier Science Publishers, B.V., Amsterdam

Stein CL (1985) Mineralogy in the waste isolation pilot plant (WIPP) facility stratigraphic horizon. SAND85-0321. Sandia National Laboratories, Albuquerque

Stormont JC, Daemen JJK (1992) Laboratory study of gas permeability changes in rock salt during deformation. Int J Rock Mech Min Sci Geomech 29(4):325–342

Stormont JC, Finley RE (1996) Sealing boreholes in rock salt. In: Fuenkajorn K, Daemen JJK (eds) Sealing of boreholes and underground excavations in rock. Chapman and Hall, London, pp 204–209. doi:10.1007/978-94-009-1505-3

Sweet JN, McCreight JE (1979) Thermal conductivity of rocksalt and other geologic materials from the site of the proposed waste isolation pilot plant. SAND79-1134. Sandia National Laboratories, Albuquerque

Urquhart A, Bauer S (2015) Experimental determination of single-crystal halite thermal conductivity, diffusivity and specific heat from – 75 to 300 °C. Int J Rock Mech Min Sci 78:350–352. https://doi.org/10.1016/j.ijrmms.2015.04.007

van den Broek WMGT (1982) Impurities in rock-salt: consequences for the temperature increases at the disposal of high-level nuclear waste. PB-83-102087. Technische Hogeschool Delft, Netherlands

von Berlepsch T, Haverkamp B (2016) Salt as a host rock for the geological repository for nuclear waste. 1811-5209/16/0012-0257$2.50. Elements, vol 12, pp 257–262. https://doi.org/doi:10.2113/gselements.12.4.257

Woodside W, Messmer JH (1961a) Thermal conductivity of porous media. I. Unconsolidated sands. J Appl Phys 32(9):1688–1699

Woodside W, Messmer JH (1961b) Thermal conductivity of porous media. II. Consolidated rocks. J Appl Phys 32(9):1699–1706

Yang JM (1981) Thermophysical properties. In: Gevantman LH (ed) Physical properties data for rock salt. Monograph 167. National Bureau of Standards, Washington, pp 206–212